Using Abaqus/CAE and User-Defined Material Subroutines to Predict the Deformations of a Stitched Triaxial Fabric during Forming Processes

Cynthia J. Mitchell, James A. Sherwood*, Lisa M. Dangora, and Jennifer L. Gorczyca

Department of Mechanical Engineering, University of Massachusetts Lowell, One University Ave., Lowell, MA 01854, USA

Abstract: *The use of a stitched triaxial fabric in composite forming applications is investigated. The fabric of interest consists of three layers of stitched fibers, which were originally oriented at [-60°/0°/60°]. The tensile, shear, and frictional behavior was investigated experimentally. Conventional shear frame testing methodology assumes that the yarns are intially mutually perpendicular. This assumption is not valid for this particular fabric geometry and must be adjusted accordingly. The determined material behavior was implemented into a user-defined material subroutine within a discrete mesoscopic finite element model built in Abaqus/CAE. Different element types were investigated to represent the fabric and determine ideal mesh configurations to best capture the mechanical behavior of the fabric. Different modes of deformation were also studied, and the observed experimental deformations were compared to the deformation predicted by the finite element model.*

Keywords: *Composites, Design Optimization, Fabrics, Forming*

1. Introduction

During the forming of a fabric-reinforced composite structure, the yarns deform to allow the fabric to conform to the curvature of the mold causing possible defects and a change in material properties. Previously, a method was developed to model the forming of woven-fabric reinforced composites. The model has the potential to investigate the effects of variations in the processing conditions used in the manufacture of the composite parts on part quality. The model as depicted in Figure 1 consists of one-dimensional and two-dimensional elements used to represent the fabric (Jauffrès *et al.*, 2009).

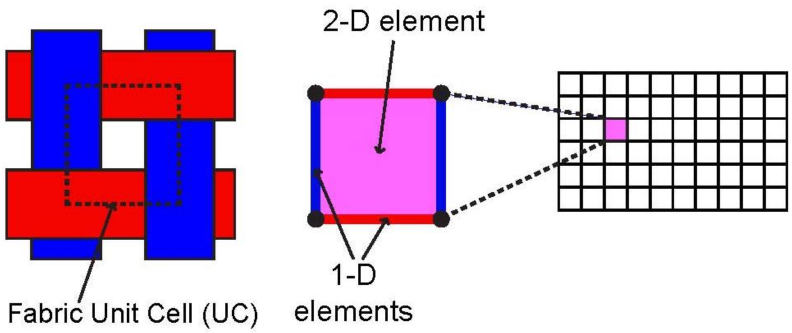

Figure 1. Fabric unit cell model (Jauffrès *et al.*, 2009).

Previous research demonstrated that this model could be used to simulate the forming of many composite parts including wind turbine blades and various automotive structures as shown in Figure 2. This figure shows the fabric after it has been deformed into the part mold. Details about the characterization of the mechanical behavior of the fabric are given in (Fetfatsidis *et al*, 2012).

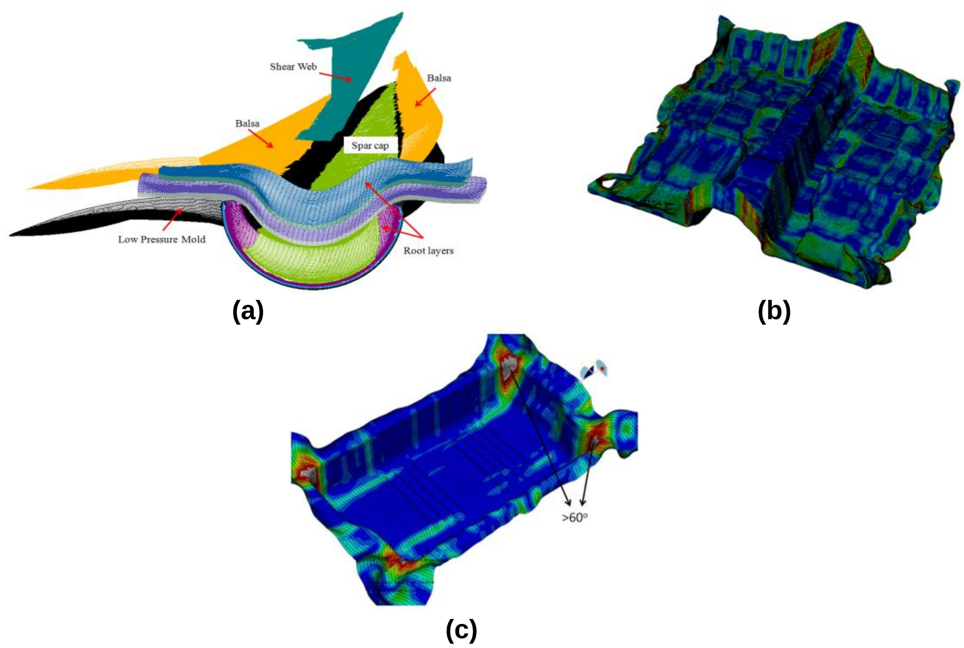

Figure 2. FE forming models of (a) half of a wind turbine blade, (b) car floor pan, and (c) a rear tub (Fetfatsidis *et al*, 2012).

Non-crimp fabrics (NCFs) are becoming increasingly popular in the composites industry. The benefit of NCFs over woven fabrics is the absence of the tow waviness that is associated with a woven fabric. The undulations of the tows results in a load-carrying path that is not as efficient as that available in an NCF. In particular, biaxial and triaxial NCFs are being used as preforms because the combination of multiple layers into a single layer can reduce cost and production times seen in manual hand layups of composites (Kong *et al*., 2004).

Kong *et al*. (2004) performed bias extension tests on a [-45°/0°/+45°] triaxial fabric to investigate the shear properties of the NCF in comparison to a similar plain-weave fabric. The observed shear deformation of the area of interest is shown in Figure 3. While the ±45° yarns shear relative to one another, the 0° yarns see very little deformation.

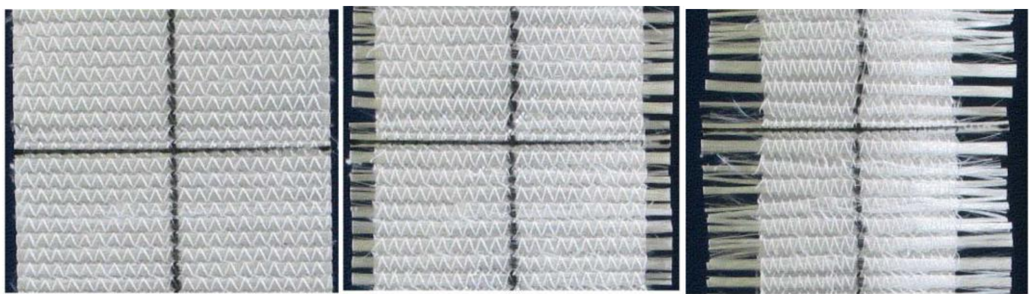

Figure 3. Observed fabric deformation during ±45° bias extension test (Kong *et al*., 2004).

In this research, the fabric of interest is a [-60°/0°/60°] stitched fiberglass fabric. This paper will focus strictly on the modeling of this fabric and will not cover any mechanical testing. The mechanical testing will be covered in a future publication.

2. Finite Element Model Description

The finite element model used to model the triaxial fabric is a mixed-mesh mesoscopic model. Beam elements were utilized to represent the tensile properties of the fabric tows, while shell elements were used to represent the shear stiffness of the fabric.

2.1 Mesh

The original mesh used to describe the fabric was a modified version of the mesh used by (Jauffrès *et al*., 2009) as shown in Figure 1. A triangular shell element modeled the shear stiffness and was surrounded beam elements to model the tensile properties of the fabric tows. Figure 4 shows the original mesh used to model the triaxial fabric. This model assumes a pin-joint boundary condition at each of the stitch locations in the fabric. Kong *et al*. (2004) demonstrated that during shearing between two sets of fabric tows, there is large fiber sliding (Figure 3), implying that the pin-joint boundary condition may not be a valid assumption for the fabric under consideration in this paper.

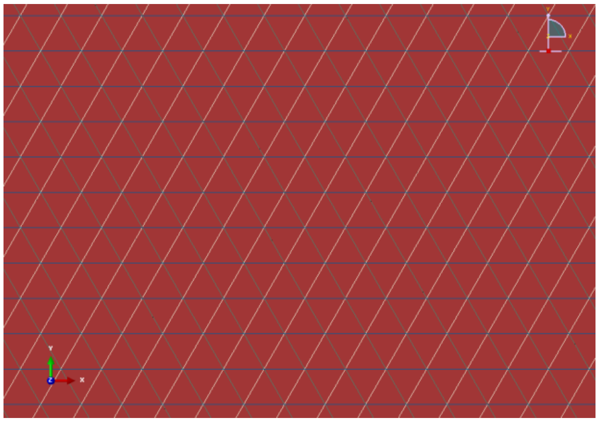

Figure 4. Original fabric mesh.

An additional mesh, referred to as a checkerboard mesh, was developed to avoid the pin-joint assumption at the stitch locations. This model was inspired by the approach developed by Sidhu *et al*. (2001) for plain-weave fabrics. The checkerboard mesh adapted to model a triaxial fabric is shown in Figure 5. This mesh replaces the one shell element with four shell elements depicted in Figure 1. Additionally, the beam elements do not share nodes with beam elements that do not represent the same fiber tow, allowing the yarns to slip relative to one another.

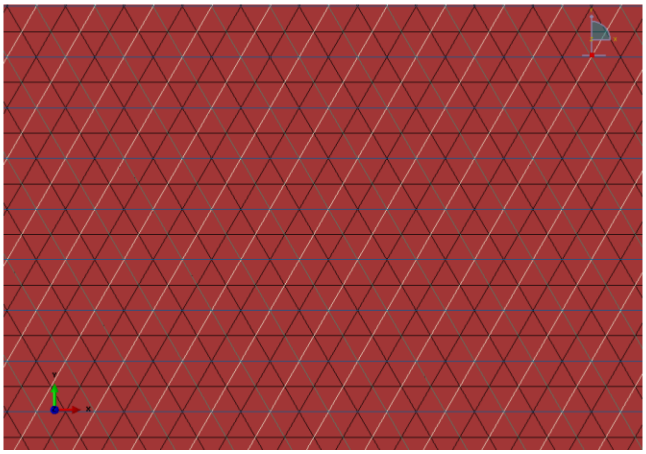

Figure 5. Checkerboard mesh configuration.

2.2 User-Defined Material Subroutine

To model large deformation and strains in Abaqus/Explicit, rate-dependent constitutive equations, also called hypoelastic laws, were used. Stresses were updated using the Hughes and Winget formula (Bathe, 1996) and are shown in Equations (1) and (2).

$$\sigma_{ij}{}^{t+1} = \sigma_{ij}{}^{t} + \Delta\sigma_{ij}{}^{t+1} \tag{1}$$

$$\Delta\sigma_{ij}{}^{t+1} = C_{ijkl} \cdot \Delta\varepsilon_{kl}{}^{t+1/2} \tag{2}$$

where $\Delta\sigma_{ij}{}^{t+1}$ is the increment of the stress tensor at time step $t+1$, C_{ijkl} is the constitutive matrix and $\Delta\varepsilon_{kl}{}^{t+1/2}$ is the midpoint increment of the strain tensor obtained from the integration of the strain rate tensor.

Abaqus/Explicit allows the linking of custom constitutive models with the overall solver to update the stress (Equation 2) via user-defined material subroutine, VUMAT. The strain increments tensor, $\Delta\varepsilon_{kl}{}^{t+1/2}$, was given by the solver to VUMAT, which subsequently returned the corresponding stress increment to the solver. The stress update was made in the local reference frame for the element, i.e. a co-rotational frame that rotates with the element (Figure 6). The summation of the strain increments gave a logarithmic (or true) strain in the principal-stretch directions (Abaqus, 2006). Details associated with the constitutive equations as they pertain to the 1-D and 2-D elements are provided in (Jauffrès *et al*., 2009). This approach assumed that that the yarns were initially mutually perpendicular. To accommodate the fabric geometry of the triaxial fabric, the approach was generalized such that e_i^0 were not necessarily equal to g_i^0. Instead, g_i^0 was oriented parallel to the initial orientations of the fabric tows and is centered within e_i^0.

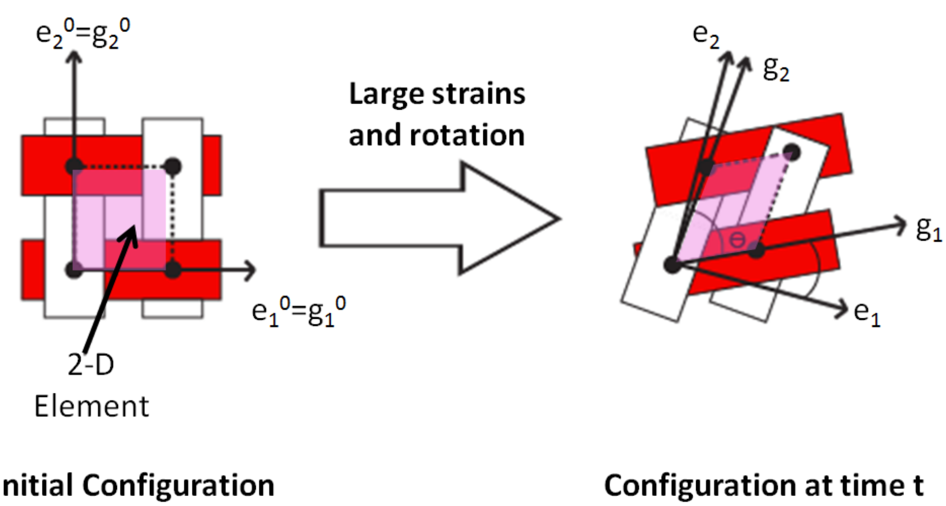

Figure 6. Schematic representation of the different coordinate systems used (Jauffrès *et al*., 2009).

3. Shear Frame

Traditional shear-frame tests consist of fabric clamped into a frame (Figure 7) with the yarns initially mutually perpendicular and parallel to the sides of the frame. The cross-yarns were removed in the arms of the specimen to ensure pure shear occurs in the area of interest (Cao *et al*., 2008).

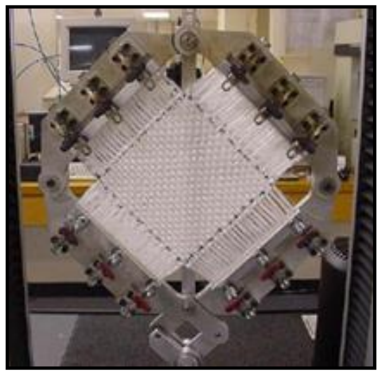

Figure 7. Shear frame test setup.

By applying a load in the bias direction of the fabric, the shear frame test applies a pure shear load on the fabric. The hinges on the corners of the picture frame allow the sides to rotate freely. Load-displacement curves are generated from the test. Typically, the load is low, but when the fabric approaches a characteristic locking angle, there is a sharp increase in load (Figure 8). Once the locking angle is reached, the fabric wrinkles out-of-plane.

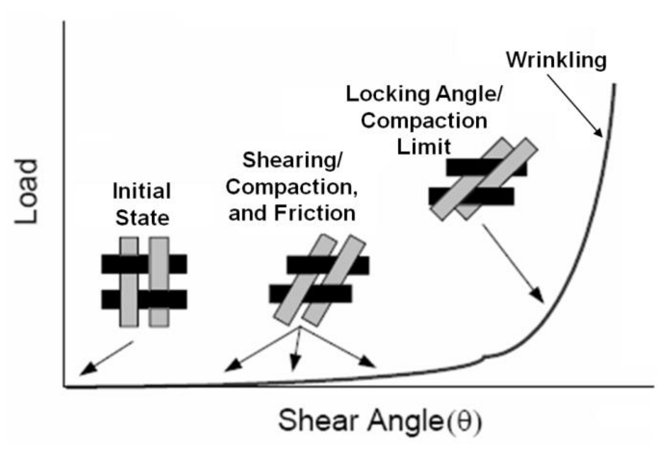

Figure 8. Typical load-shear angle curve for a shear-frame test (Lussier, 2002).

Due to the fabric geometry, it was not possible for the tows to be originally perpendicular to each other. Instead, the frame was extended to accommodate the initial orientation of the ±60° yarns, and the 0° yarns remained unconstrained. The model for the shear frame is shown in Figure 9. The top of the frame was displaced to induce approximately 15° shear in the fabric. The shear-frame model was run for the different mesh patterns introduced in the previous section. The results were compared to an empirical curve derived from the shear properties implemented in the model.

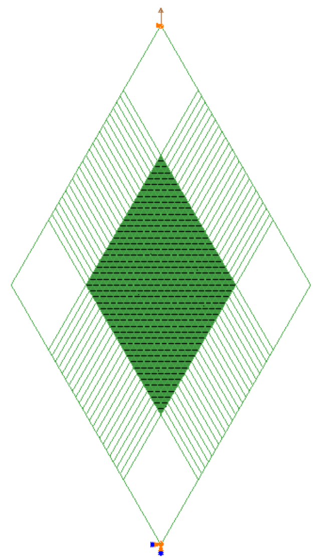

Figure 9. Shear frame model modified to accommodate triaxial fabric geometry.

3.1 Original Mesh

When the pinned-joint assumption was implemented between the intersecting yarns, the fabric was unable to shear due to the fabric geometry. Unlike the biaxial fabrics, the triangular unit cells did not allow shearing due to the stability of the triangular geometry. Figure 10 shows the model in its deformed configuration. Instead of shearing, the area of interest simply rotated about the arms. As a result, the shear angle (SDV3) is much lower than the expected shear angle of 15°.

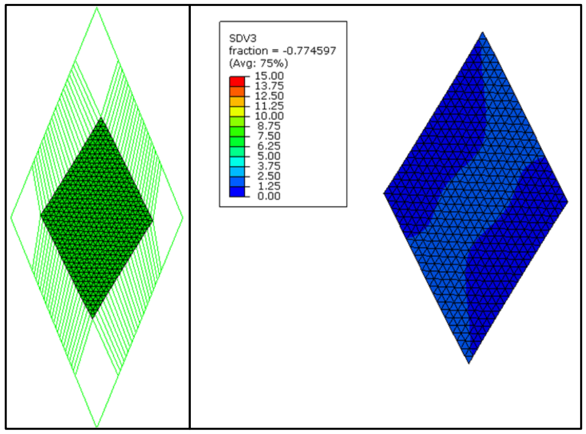

(a) (b)

Figure 10. (a) Shear frame deformation and (b) shear angle in the region of interest.

3.2 Checkerboard Mesh

The checkerboard mesh allowed the fabric to shear because it did not impose a pin-joint assumption on the yarns. However, as the corners of the region of interest contracted, the yarns in the 0° direction were compressed to conform to the change in geometry, causing out-of-plane buckling of the yarns as seen in Figure 11.

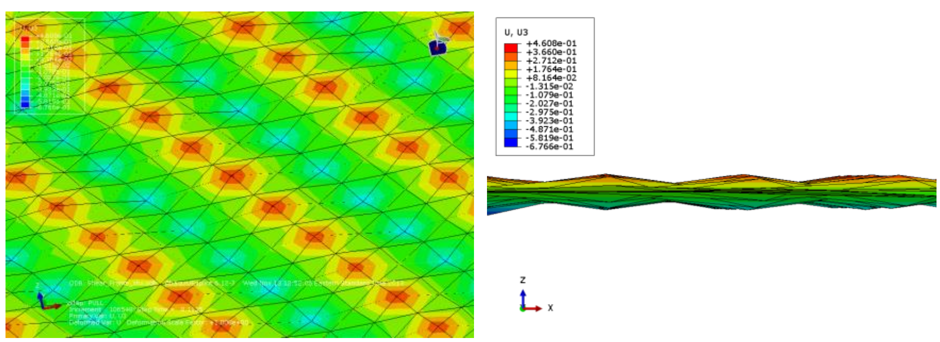

(a) **(b)**

Figure 11. Egg-crate mesh instability in checkerboard model (a) front view and (b) side view

3.3 Biaxial Mesh

To allow the fabric to shear, the 0° yarns were removed from the original mesh, essentially creating a ±60° biaxial fabric. The results of the shear-frame test showed that the model successfully followed the prescribed load-displacement curve indicating that the user-defined material subroutine for the shell elements was being implemented correctly (Figure 12). Thus, the S3 elements can potentially work as well as the S4 elements for this mesoscopic approach to model the fabric.

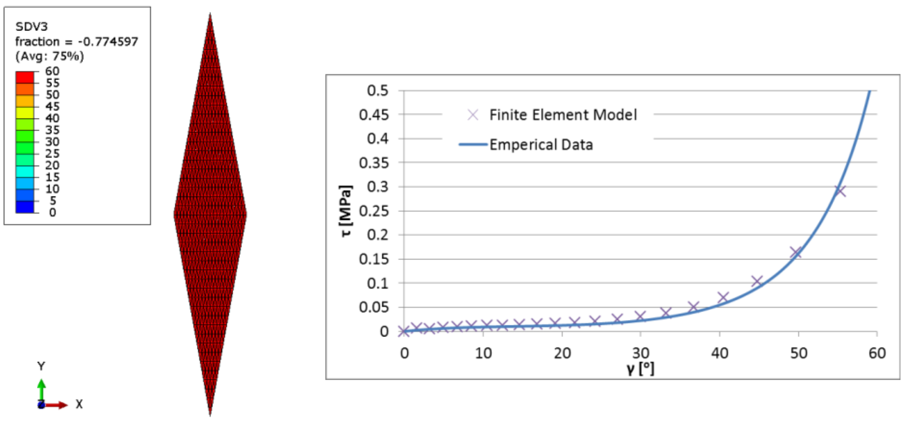

Figure 12. Shear frame results of ±60° biaxial fabric model.

4. Conclusions

A stitched [-60°,0°,+60°] fabric was investigated using the finite element method where the shear behavior of the fabric was modeled using shell elements and the tows were modeled using beam elements. One mesh assumed a pin-jointed behavior for the crossover points of the yarns, and the other mesh used a checkerboard approach that allowed relative yarn sliding. The checkerboard model produced a theoretically more realistic response.

5. References

1. Abaqus I. Abaqus Theory Manual Version 6.6-1: Abaqus, Inc., 2006.

2. Bathe K. J., Finite Element Procedures. Englewood Cliffs: New Jersey: Prentice Hall, 1996.

3. Cao, J., Akkerman, R., Boisse, P., Chen, J., Cheng, H.S., DeGraaf, E.F., Gorczyca, J., Harrison, P., Hivet, G., Launay, J., Lee, W., Liu, L., Lomov, S., Long, A., Deluycker, E., Morestin, F., Padvoiskis, J., Peng, X.Q., Sherwood, J., Stoilova, T., Tao, X.M., Verpoest, I., Willems, A., Wiggers, J., Yu, T.X., Zhu.: "Characterization of mechanical behavior of woven fabrics: experimental methods and benchmark results", *Composites: Part A*, **39,** pp. 1037-1053, (2008).

4. Fetfatsidis, K.A., Soteropoulos, D., Petrov, A., Mitchell, C.J., and Sherwood, J.A.: Using Abaqus/Explicit to Link the Manufacturing Process to the Final Part Quality for Continuous Fiber-Reinforced Composite Fabrics. Simulia Community Conference, 2012.
5. Jauffrès, D., Sherwood, J.A., Morris, C.D., and Chen, J.: “Discrete mesoscopic modeling for the simulation of woven-fabric reinforcement forming” *International Journal fo Forming*, Volume 3, Supplement 2, p.1205-1216, 2009.
6. Kong, H., A.P. Mouritz, and R. Paton, Tensile extension properties and deformation mechanisms of multiaxial non-crimp fabrics. Composite Structures, 2004. 66(1–4): p. 249-259.
7. Lussier, D.: Shear characterization of textile composite formability, MS Thesis, Department of Mechanical Engineering, University of Massachusetts Lowell, 2002.
8. Sidhu, R. M. J. S., Averill, R. C., Riaz, M. and Pourboghrat, F.: “Finite element analysis of textile composite preform stamping,” Composite Structures 52, pp. 483-497, 2001.

6. Acknowledgements

The authors would like to acknowledge the National Science Foundation for its support of this research through Award No. 1230884.